iJRASET
International Journal For Research in Applied Science and Engineering Technology

INTERNATIONAL JOURNAL FOR RESEARCH

IN APPLIED SCIENCE & ENGINEERING TECHNOLOGY

Volume: 13 **Issue:** V **Month of publication:** May 2025

DOI: https://doi.org/10.22214/ijraset.2025.70494

www.ijraset.com

Call: 08813907089 | E-mail ID: ijraset@gmail.com

International Journal for Research in Applied Science & Engineering Technology (IJRASET)
ISSN: 2321-9653; IC Value: 45.98; SJ Impact Factor: 7.538
Volume 13 Issue V May 2025- Available at www.ijraset.com

Recent Inter-Seasonal Variability of EDW in the North Atlantic using Volume Index

Sonfack Brice Rousvel[1], Komkoua Mbienda A. J[2], Guy Merlin Guenang[3], Kenfack-Sadem Christian[4], Mpame Guilène[5], Nzeukou Armand[6], Vondou Appolinaire Derbetini[7]

[1,6]*Research Unit of Engineering of Industrial Systems and Environment (RU-EISE), IUT-FV, University of Dschang, PO BOX 134 Bandjoun, Cameroon*

[2,3]*L2MPS, Department of Physics, Faculty of Science, University of Dschang, Dschang, Cameroon.*

[3,7]*Laboratory for Environmental Modeling and Atmospheric Physics (LEMAP), Faculty of Sciences, University of Yaoundé I, and PO BOX 812 Yaoundé, Cameroon*

[4]*Condensed Matter Physics and Nanomaterials (CMPN), Faculty of Sciences, University of Dschang, PO BOX 134 Bandjoun, Cameroon*

[5]*Laboratoire d'Automatique et d'Informatique Appliquée (LAIA), IUT-FV, University of Dschang, PO BOX 134 Bandjoun, Cameroon*

Abstract : ***The inter-annual, intra-seasonal, and seasonal variability of Eighteen Degree Water (EDW) volume was investigated in this paper using a metric called the Volume Index (VI), based on the vertical integration of the oceans layer probability to have a temperature in the Mode Water range over a given time range t. Our main objective was to quantify and compare the total volume of EDW in the winter and summer. This method has been applied to BOA-Argo datasets from 225,792 existing temperature profiles for the period 2004-2019 over the subtropical North Atlantic region and sought to capture the variability of EDW volume. Monthly North Atlantic Oscillation (NAO) data from CRU and ENSO data from PSL-NOAA have also been used and compared to the trend of the EDW volume variability to understand its cause. We have analyzed the total volume of EDW during winter (JFM) and summertime (JAS) and compared their signals, and the major results of this paper demonstrate that the total volume of EDW is more important in summer (JAS) than in winter (JFM). We found that EDW total volume illustrated a significant anti-correlation with NAO in the summer. Our study has shown the EDW total volume fluctuates around 60 Svy, reaching its maximum at 72 Svy. In addition, the EDW total volume fluctuates around 65 Svy with values varying between 55 and 72 Svy in summer, while it is around 52 Svy with values varying between 41 and 106 Svy in winter. The interannual variability brought out a slight increase from 2004 to 2008, a signal oxalate around a stable level from 2008 to 2014, and a remarkable downward trend during 2014-2017. The Volume Index (VI) displayed a good stratification of EDW in the ocean. NAO correlates well with the noticeable downward trend in EDW volume during 2015-2017. Intra-seasonal variability also showed the same downward trend in both winter and summertime. We also observed the weak signal of the EDW volume during the winter season of 2011, which is also well correlated with El Niño 2009-2011. Finally, the metric VI, the method of VI proved to be an efficient analysis tool to capture the variability of EDW volume with a statistical uncertainty of around 0.1.***

Keywords: EDW, Volume variability, inter-annual, intra-seasonal, Probability, Temperature profile, Volume index.

I. INTRODUCTION

Subtropical Mode Water (STMW) is upper ocean water masses with nearly uniform temperature and salinity over a thickness of hundreds of meters that is found over a relatively large geographical area (subtropical gyres). It is located on the warm side of a Western Boundary Current (WBC) and is a common feature of the subtropical gyres in the North Atlantic and the North Pacific. It is found at the pycnostad and usually occurs between the permanent pycnocline and the seasonal pycnocline [1-3]. It is formed in winter via convective mixing driven by heat loss to the Atmosphere [4-7] on the warmer side of separated western boundary currents such as the Gulf Stream and Kuroshio [1, 8-12]. The surface of the ocean below where STMW is formed constitutes an interface of exchange of gases and heat with the atmosphere and plays an important role in the stability of the climate by regulating the rate of CO2 in the atmosphere [13-15] through the injection of water into the thermocline each winter.

The study of the variability of STMW implies recognizing the substantial encompassed volume and how it fluctuates from year to year. The homogeneity of temperature, salinity, and oxygen in the horizontal and vertical water columns are used to localize the STMW volume.

Many authors investigated the variability of STMW based on mapping and interpolation methods and models. Fernandez [16] studied the variability of STMW in the Southwest Pacific. The Roemmich-Gilson [11]optimal interpolation method was used on monthly Argo over 28 years, and they showed that the STMW volume is correlated with negative anomalies in surface heat fluxes. In addition, the investigation of the variability of STMW was carried out using reanalysis and mathematic models [6, 7, 17-19]. Using the mapping method, [20] examined the mean annual cycle and long-term variability of North Atlantic Subtropical Mode Water (NASTMW) over a 40-year period (1961-2000). Their Results illustrated an interannual to-decadal cycle that is strongly correlated to the North Atlantic Oscillation (NAO) index. We are interested in the variability of the volume of NASMW also called Eighteen Degree Water (EDW). A metric based on the vertical integration of the oceans layer probability is used in this study to capture the substantial volume of EDW. This metric has the advantage to capture the variability of the EDW based on the temperature. EDW volume exhibits a low-frequency variability but it is very difficult to observe because of the very large amplitude of the seasonal cycle. Therefore, it is crucial to be able to monitor the volumetric census of EDW and to estimate associated error bars. In this note, we present a simple metric to monitor in time the volume of EDW. This metric is in fact a proxy of the volume variability, i.e. it cannot be linked directly to the absolute amplitude of the volume. Only the variability is captured.

A large number of studies have investigated the EDW; [21] studied EDW variability in Western North Atlantic; [22] analyzed STMW in the 137°E section. Furthermore, [20] investigated the seasonal variability of NASMW; observation of the cycle of convection and restratification over the Gulf Stream was made by the Climode Group (2009; 2019); [5] used transformation and formation maps to study the role of air-sea heat fluxes in north Atlantic eighteen degree water formation; [6] Estimated seasonal cycle of North Atlantic eighteen degree water volume. Maze carried out many studies on STMW in various forms [5, 23, 24]. More recently, the interannual and decadal variability of STMW in the North Atlantic Ocean has been studied by [25]. Many studies of the variability of EDW have been based on either the mapped or interpolation method and models. Obwohl, [25] provided a recent trend of the variability of the EDW,[6] estimated the seasonal cycle of EDW in volume formation rate and [23] estimated the seasonal cycle of the mixed layer using potential vorticity, more studies need to be done to clearly understand all the processes within EDW.

We want to illustrate another way to capture the variability of the volume of EDW using the approach introduced by [6] and [7]. Therefore, we have used a metric based on a simple analysis of Argo in-situ vertical profiles of temperature, which does not directly imply mapping or interpolation on a regular grid. It is the vertical integral of the oceans layer probability to have a temperature in the mode water range over a given time range t as done by [6] and [7] globally. Our work aims to explore the interannual and intra-seasonal variability of EDW and the difference in seasonal variability using this metric. We have analyzed the total volume of EDW during winter (JFM) and summertime (JAS) and have compared their signal. How does EDW total volume vary and what causes this variability? Can the Volume Index capture the difference in seasonal variability? What is the advantage of using this metric, Volume Index compared with another method? The plan of our work is presented as follows. In section 2, the presentation of the study area, data, and method. The result and discussion have been made in sections 3 and 4.

II. DATA, METHOD, AND STUDY AREA

A. Data

1) The BOA-Argo dataset

Argo data were collected and made freely available by the international Argo project and the national programs that contributed to it. The objective of the Argo program is to operate and manage a set of over 4000 floats distributed in all oceans, with the vision that the network will be a permanent and operational system. A typical Argo float drifts for three years or more in the ocean. It continuously performs measurement cycles. Each cycle lasts about 10 days and can be divided into 4 stages. a descent from surface to a parking pressure (e.g. 1500 decibars), a subsurface drift at the parking pressure (e.g. 10 days), an ascent from a fixed pressure to surface (e.g. 2000 decibars), and a surface drift with positioning and data transmission to a communication satellite (e.g. 8 hours). Profile measurements (e.g. pressure, temperature, salinity) are performed during ascent, occasionally during descent. Subsurface measurements during parking are sometime performed (e.g. every 12 hours). The Argo data system has three levels of quality control. The first level is the real-time system that performs a set of agreed automatic checks on all float measurements. Real-time data with assigned quality flags are available to users within the 24-48 hours timeframe, the second level of quality control is the delayed-mode system, and the third level of quality control is regional scientific analyses of all float data with other available data.

The new dataset, Barnes Objective Analysis (BOA-Argo) data, which is data quality control, is used in this paper. It is an Argo temperature and salinity data set from 2004 to 2019, with monthly temporal resolution and a 1° x 1° horizontal grid. The BOA-Argo dataset contains 49 vertical levels from the surface to 1950 m depth [26].

The gap observed in the different graphs comes from computations. The BOA-Argo dataset is slightly better than other gridded Argo data sets produced using Optimum Interpolation (OI) such as variational analysis [26]. Since it can retain more mesoscale features than other gridded Argo data sets.

2) NINA 3.4 data

The El Niño-Southern Oscillation (ENSO), is the interannual variation of the atmosphere-ocean system in the equatorial Pacific which has three phases. warm (El Niño), cold (La Niña), and Neutral. Although El Niño is considered the warm phase of ENSO and La Niña the cold phase, they are not considered opposites because they occur with differing magnitudes, spatial extent, and duration. Impacts of ENSO stretch far beyond the region through interactions called teleconnections. El Niño brings warmer-than-average waters to the central and eastern tropical Pacific, sometimes to the coast of South America. At the surface, the prevailing easterlies (the trade winds) slow down, or sometimes even reverse. La Niña brings cooler-than-average waters to the central and eastern tropical Pacific, again, sometimes all the way to South America. The prevailing easterlies intensify. Neutral means neither El Niño nor La Niña conditions is present in both the ocean and the atmosphere. Sometimes "neutral" genuinely means that conditions in the ocean and the atmosphere are near average. Niño 3.4 data come from the equatorial Pacific Ocean (5°N-5°S and 170°W-120°W), calculated from the PSL HadISST1 dataset. It is monthly anomaly data from 2004- 2021 and area-averaged Sea Surface Temperature (SST) anomalies from 5°S-5°N and 170°-120°W. The Niño 3.4 index typically uses a 5-month running mean, and El Niño or La Niña events are defined when the Niño 3.4 SSTs exceed + /-0.5°C for six months or more. ENSO is one of the most important climate events, which can change global circulation, which then has an impact on global temperatures and precipitations.

3) NAO data

The NAO index is a weather phenomenon over the North Atlantic Ocean, based on the surface Sea-Level Pressure (SLP) Variations between the Subtropical (Azores) High and the Subpolar (Icelandic) Low. The variations in the strength of the difference of pressure between the high pressure in the Azores and low pressure in Icelandic can drive changes in atmospheric conditions over North Atlantic Subtropical gyre and lead EDW ventilation [20]. Therefore, the analysis of the correlation between the periodicity of NAO and EDW can help to understand its variability. NAO index is monthly data from 2004-2021 provided by CRU.

B. Method

Here, an objective method has been developed for the characterization of EDW from Argo profiles. It is based on two criteria.

- The Selected temperature profiles must be in the EDW range, i.e. between 17 and 19 degrees Celsius.
- Profiles thickness, which is the difference of the depth corresponding to these two temperatures 17 and 19, must be greater than 20 m.

$H = depth(17) - depth(19) > 20$

Only profiles satisfying both criteria are considered as belonging to the EDW region [18°N-42°N, 84°W-35°W] were selected.
In order to compute and study the interannual and seasonal variability of EDW volume, Volume Index has been assessed focusing on the vertical integration of the oceans layer probability. This metric is solely based on a simple analysis of in-situ vertical profiles of temperature. It does not imply complex mapping or interpolation on a regular grid. We call this metric V and define it as the vertical integral of the oceans layer probability to have a temperature in the mode water range over a given time range t.

$$\hat{V}(t) = \frac{1}{H}\sum_{k=1}^{N_z} p(t,k)\, dz(k) \qquad (1)$$

Where H is the total sampling depth, i.e. the sum of all layers thickness dz. The probability $p(t; k)$ is the probability for a water parcel temperature in the pre-defined layer k of thickness $dz(k)$ to be in the range of the mode water. It is thus given by.

$$p(t,k) = \frac{1}{N_p^k}\sum_{p=1}^{N_p^k} \delta\,(k,p) \qquad (2)$$

Where $Nk;p$ is the number of samples available in layer k and $\delta(k; p)$ is the water mass mapping function. it is one if the temperature $T(k; p)$ in layer k of profile p is in the range defining the mode water and zero otherwise. This is simply the ratio between the number of mode water samples with the total number of samples.

Note that we consider that one profile provides no more than one sample for each layer. A lower bound of the error associated with $p(t; k)$ can be computed if we consider all samples of a given layer to be independent realizations of a random variable. This would be the case if the region considered is large enough. This error is given by.

$$e(t,k) = \frac{\sigma_\theta^k}{\sqrt{N_p^k}} \quad (3)$$

Where k is the standard deviation of temperature samples in layer k. As pointed out by Gatz and Smith [27, 28], there are no rigorous formulae to estimate the standard error on a weighted mean such as $V(t)$. So here, we choose to use.

$$\hat{E}(t) = \frac{1}{H}\sqrt{\sum_{k=1}^{N_z} e(t,k)^2\, dz(k)^2} \quad (4)$$

Note that this estimate tends toward the standard error on the mean if all layers have a similar thickness. If the entire domain of analysis is filled with mode water, the probability p will be 1 at each layer, and $V(t) = 1$. On the opposite, if no mode water is found in the domain, the probability p is null at each layer, and $V(t) = 0$. Our working hypothesis is that even using a limited number of vertical profiles, in an appropriately chosen region of the ocean $V(t)$ will be able to capture the temporal variability of the mode water true volume in that region. The true normalized volume of mode water in a given region of the ocean can be computed as.

$$(t) = \frac{1}{V_\mathcal{R}} \sum_{\mathcal{X}=1}^{n_\mathcal{X}} \sum_{\mathcal{Y}=1}^{n_\mathcal{Y}} \sum_{\mathcal{Z}=1}^{n_\mathcal{Z}} \mathcal{H}(\mathcal{X},\mathcal{Y},\mathcal{Z},t)\, dV(\mathcal{X},\mathcal{Y},\mathcal{Z}) \quad (5)$$

where VR is the total volume of the region, H is the mode water mapping function (1 if the temperature at location (x; y; z; t) is in the range defining the mode water and 0 otherwise), and dV volume elements. This is a simple sum of the points where the temperature is in the range defining the mode of water, each point being weighted by a volume element. Similarly, to the estimator $V(t)$, the true volume fraction of mode water $V(t)$ is one if the region is filled with mode water and zero if no mode water is found.

C. Study Area

The study area stands in the subtropical gyre of midlatitude in the North Atlantic Ocean and extends between latitudes 18°N and 42°N and longitudes 84°W and 35°W (Fig.1). Its main characteristic is the western boundary current, the Gulf Stream (GS), which transports heat along the North Atlantic Ocean. It is a zone of deep convection during the winter when cold and dry air outbreaks near the continent (southwest of Europe) cold down the surface water masses and generate the convection process under the ocean and formation of North Atlantic subtropical mode water [4, 24].

III. RESULTS

A. Characteristics of Subtropical Mode Water

The development of BOA-Argo data has been delivered for easier use of ocean data. It makes the study and analysis of ocean data easier. Since it includes a good part of data profile processing in the ocean. The method of EDW characterization was exposed in section 2.2. It holds essential information to monitor the study and analyze the variability of EDW. This method is applied to BOA-Argo datasets from all

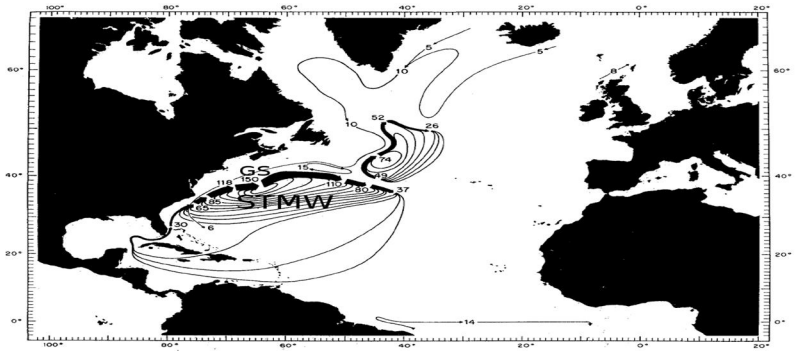

Fig. 1. Study area (coordinates [18°N-42°N, 84°W-35°W]), the Subtropical North Atlantic with its mean features, the western boundary current, the Gulf-Stream (GS), the subtropical gyre of mid-latitude and the Subtropical Mode Water (STMW) just south of Gulf Stream from Worthington (1976), isolines correspond barotropic current function.

Existing profiles for the period 2004-2019 over the study area. All profiles containing Eighteen Degree Water were selected as a result of this method and represented. Figure 2.a shows the EDW temperature profiles, which is defined as profiles containing temperature within 17 and 19 degree Celsius over the study area and whose thickness between both layers containing these temperatures is greater than 20m. All the temperature profiles during the period 2004-2019 were plotted. Out of 225,792 initial BOA-Argo profiles from January 2004 to December 2019 throughout the study area, 172,477 temperature profiles were selected respecting the EDW criteria in our study. Around 200m depth and near the surface, there are global profiles whose temperature decreases rapidly from 27° to 19°C with the depth, these correspond to the seasonal thermocline. Between 200 and 600m depth, there is a place, where the temperature is almost constant around 18°C, forming a nearly isothermal layer or thermostad [29], this is the EDW core. From 600m to 1200m temperature decreases less rapidly with depth, this is a permanent thermocline. From 1200m to 2000m, the temperature is almost stable. The maximum temperature reaches 32°C on the surface and the minimum temperature is 3°C at the bottom (2000 m depth). The seasonal thermocline obtained near 200 m is located on the top of EDW. It forms in spring and summer and disappears during winter cooling when water is exposed to surface cooling and therefore loss of buoyancy [30]. However, the main thermocline observed between 600m and 1000m persist throughout the year and is found at bottom of EDW [1]. We can see from figure 2.a that it moves up and down from nearly 500m to a proximity of 1000m depth. One of the reasons would be the variation of the profile with the time and space.

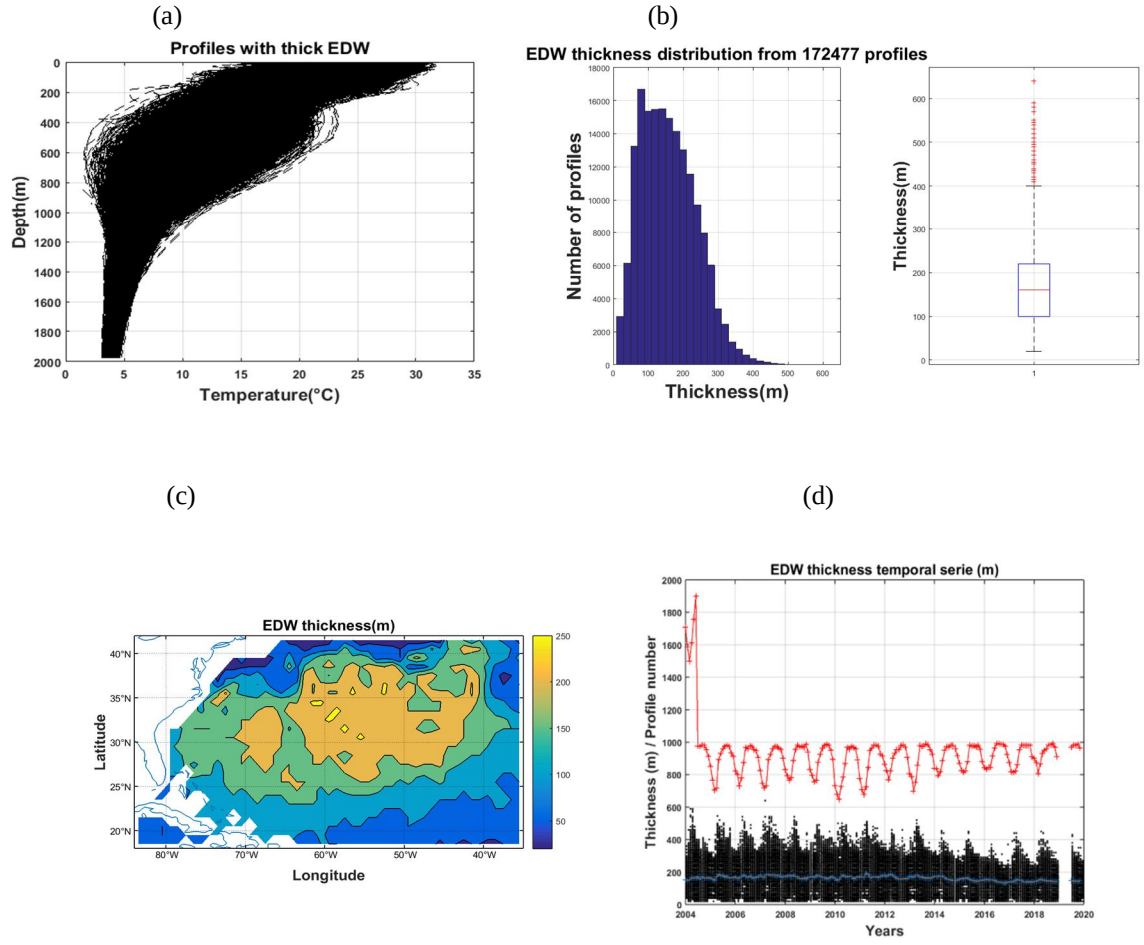

Fig. 2. Characteristics of EDW in the Subtropical North Atlantic and EDW thickness temporal series from January 2004 to December 2019. (a) Eighteen Degree Water temperature profiles from the period 2004-2019 with thick greater than 20m over the study area (18°N-42°N, 84°W-35°W), (b) EDW thickness histogram distribution of the temperature profiles from 2004 to 2019, (c) EDW thickness and geographical position from 172477 profiles during the period 2004-2019. (d)Monthly mean timeseries of profile numbers (red line), monthly mean of EDW thickness (blue line), and initial profiles (black scatter plot).

As matter of fact, the main thermocline is deeper in winter than the rest of the year due to surface cooling and convection process during this time. Also, the characteristic of surface water over the study area is not the same throughout. The isothermal layer (around 18°C) between 200m and 600m is homogeneous water called Eighteen Degrees. It is found between the main thermocline and seasonal thermocline [1-3], and is formed and renewed each winter by convection. This constitutes the main characteristic of the EDW that we are going to use for the study of interannual variability.

The histogram of EDW thickness distribution displayed a normal probability density (Figure2.b), which reach the top around 180 m. Statistics have shown that the largest EDW thickness is around 640 m and the smallest is 20m. EDW thicknesses around 180m have taken the majority part of the profile number with its maximum at 15500 profiles. Only a few numbers of profiles have thicknesses around 500m. Histogram shows well that most profiles distribution have thicknesses in the range of 100-200m with a mean of 180m. EDW thickness and geographical position were also mapped from the above selected and represented temperature profiles for a more comprehensive characteristic of EDW.

It was obtained by computing the difference between layers of temperature 17°C and 19°C for each profile of the period 2004-2019 over the study area.

Then, EDW thicknesses were averaged over the time period of our study for each geographic position. It is displayed in figure2.c the information on the average thickness of EDW for each geographical position from 172,477 BAO-Argo profiles over the study area. All profile thicknesses from January 2004 to December 2019 have been averaged and plotted. EDW thickness peaks at 260 m just south of Gulf Stream, particularly between longitudes 50°W and 65°W and latitudes 30°N and 36°N. This thickness decreases rapidly to 100 m from 48°W in the East, and slightly to 50 m from 30°N in the south. We note a front on the Gulf Stream side, where the thickness decreases deeply to 0, explaining the fact that there is no EDW on the north side of the GS. It is shown on this graph just south of GS that the thickness is much larger than the whole (overall).

This could be explained by deep convection which occurs mainly during the winter when water bodies are cooling down. One of the important characteristics of this zone is the higher heat [10]. In fact, surface water bodies are warmer on the south side of GS than on the north.

Thus during the winter, there is a lot of heat loss in this (warmer) side by transfer to the atmosphere when cold and dry air cools the surface water and generates convection [10]. Figure 2.d shows the monthly time series of EDW thickness with profile, monthly average time series of profile numbers (red line) and monthly average EDW thickness (blue line), and the initial profiles (black point cloud). We can notice that the number of profiles fluctuated between 700 and 1000 profiles per month in the study area, while the EDW thicknesses revolve around 180m during the period 2004- 2019. The unimodal seasonal cycle can be observed both on the EDW thickness and on the initial profiles.

B. Interannual variability of EDW using Volume Index

Many studies have investigated the variability of EDW using various methods. In this article, we use a metric to capture the variability of EDW, which we have called the Volume Index. Here, the analysis is based on objectively mapped observations; we need a volume estimate using a volume index. In the first part of our work, we calculated the probability index of each layer (from top to bottom of the ocean at 2000m) as shown by formula (2).

The ocean is divided into several layers (Mixed or Upper Layer, Intermediate Layer, and Deep Layer). Our method modeled the ocean into several small layers and assume that there is no more than one observation for each profile in each layer grid. The monthly mean of EDW probability index and Volume for the region [18°N-42°N, 84°W-35°W] has been calculated for each layer throughout the study period.

The Volume has been derived by multiplying the probability index by the volume of each layer. Then, it has been converted unto Sverdrup per one year ($1Svy = 3.15 * 10^{13}\ m^3 = 10^6 m^3 s^{-1}$). BAO-Argo data were derived from a 1° x 1° horizontal grid, with 1° latitude and longitude corresponding to 111 km. Figure3 shows the vertical profile of the monthly mean time series of the EDW probability index (a) and Volume (b) in the region. The vertical profile of the EDW probability index and the Volume have displayed a very good similarity in patterns. We noticed as well

ISSN: 2321-9653; IC Value: 45.98; SJ Impact Factor: 7.538
Volume 13 Issue V May 2025- Available at www.ijraset.com

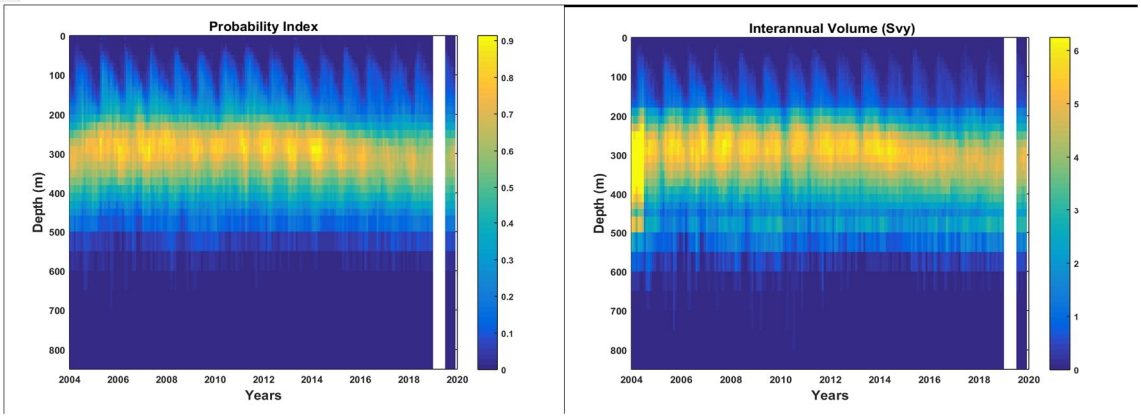

Fig. 3. Vertical profile of the monthly mean time series of the EDW probability index (a) and Volume (b) in the Subtropical North Atlantic (temporal series from January 2004 to December 2019). The Volume unit is in Svy as indicated on the colorbar, ($1Svy = 3.15 * 10^{13} m^3 = 10^6 m^3 s^{-1}$).

a good distribution of the EDW probability index as EDW Volume on the vertical profile. The distribution of the EDW probability index/volume gradually increased from the top of the ocean (with a probability/Volume of 0) to a depth of 300 m, where it reached the maximum value (0.9=6.4*Svy*), then remained almost constant between 250 and 350 m (0.8 - 0.9=5 - 6.4*Svy*) and finally decreased from 350 m to 600 m depth (0.8 - 0.1=5 - 1*Svy*). Above 600 m deep to the ocean floor, the probability/Volume is approaching zero. We also observed variability of EDW over time in the probability index and Volume. Here overall, it increased slightly from 2004 to 2008. Then, it remained almost constant during the period 2008-2014. Finally, it declined remarkably from 2014 to 2019. The graph also showed seasonal variability, where the probability index /Volume frequently reaches the minimum February-March cycle and the maximum July-August cycle of each year. The first meters of the ocean (0-150 m), where the probability index/Volume is weaker (0-0.4=0-2.5*Svy*) show the weak presence of EDW, which increases with depth. It referred to the domain where the temperature decreases rapidly with depth out of wintertime. It is the development zone of the seasonal thermocline. This is also the EDW formation domain, which took place every winter in the subtropical North Atlantic by convective mixing due to buoyancy loss of air-sea heat from the ocean surface. In fact, during the wintertime, the seasonal thermocline is destroyed due to this mixing and progressively rebuilt after this season. Then we observe the EDW core, which is in a thick band (200 - 400 m deep) with a higher probability/Volume (0.6 - 0.9=4 - 6.4*Svy*). Here, EDW is frequently present with some high proportion. It is always present in this band during the year as studied by [31, 32]. In addition, the presence of EDW decreases from 400 m to 600 m depth (0.6 - 0.1=3.9 - 0.5*Svy*). Here, it is the found main thermocline [1], which is permanent during the year. Above 700m depth, EDW presence is very rare. The probability index/Volume method illustrated well the vertical stratification of EDW in the ocean water column. Overall, the monthly average time series of the EDW probability index showed a volume that fluctuates between 0-620 m depth in the subtropical North Atlantic Ocean (latitudes 18°N-42°N and longitudes 84°W- 35°W). The core of EDW designated by the yellow zone shows a trend of inter-annual variability, which could explain a volume that increases slightly from 2004 to 2008, then is almost stable from 2009 to 2014, and finally decreases significantly from 2014 to 2019. This result is in good agreement with the work of Stevens et al. [25], who also observed a downward trend in EDW from 2014 to 2019. The brighter yellow color observed in the year 2004 (Figure 3.b) is due to the higher number of profiles present in the ocean as shown in Figure 2.d. However, it is important to note that the BOAArgo dataset is slightly better than other gridded Argo data sets produced using OI, since it can retain more mesoscale features than other gridded Argo data sets. We can well observe the signature of the seasonal thermocline on the vertical profile of the monthly mean time series of the EDW, which decays from June to March and increase from March to June, delimiting the upper mixed layer and EDW volume interior. We used the EDW probability index as a useful tool to study, analyze and estimate the weight of EDW and its Volume in each ocean layer in our study area and to capture the inter-annual variability. In the next part of our work, we used the Volume Index method to assess the variability of EDW standard total volume and true volume in the region. For this reason, we have processed formula (1) and generated the monthly average time series of the EDW Volume Index (Figure 4.a), formula (4) its error (Figure 4.b), and formula (5) the true Volume (Figure 4.c). We computed the standard EDW volume for different layers or thicknesses, from the top of the ocean 0m to 620m deep (black line), then 150-450m deep (magenta line), and finally 200-400m deep (blue line).

The three patterns show the same trend, a slight increase from 2004 to 2008, a quasi-stable trend from 2008 to 2014, and a downward trend from 2014 to 2019. The first pattern represented by the layer 0-620 m (black line) is the total standard volume of EDW with a value that fluctuates around 0.28. It is like the integration of the EDW volume in each layer over the total volume that includes all the layers in the study area. However, the total standard error of volume of the analytical expression stands around 0.1 (fig.3b). Then the volume index increases around the value 0.5 at the second pattern with a layer of 150 to 450 m, and finally the largest volume index of 0.65 at the third pattern with a layer of 200 to 400 m. We observed that the volume index is increasing, while the layer is more tightened. This simply illustrates the fact that the EDW is more present towards its core (200-400 m layer) than elsewhere. The EDW volume takes up more space in this layer than the others. The vertical profile of the probability index as well as the three patterns of Volume Index or standard volume showed an interannual variability of EDW that has three trends. Slight growth from 2004 to 2008, stability from 2008 to 2014, and a remarkable decline from 2014 to 2019. Volume Index uses a layer-weighted mean in its analytical expression, with a probability of EDW presence as a weighted point. Therefore, the results showed that its standard error fluctuates around 0.1, which corresponds to its statistical uncertainty. Across the North Atlantic, Worthington [4] estimated the annual average EDW volume by 81Svy and Forget [6] by 75Svy using the OCCA dataset. In this paper, we have used the objectively mapped BAO-Argo dataset for EDW volume estimate. The development of the BAO-Argo dataset uses a 1◦ x 1◦ horizontal grid, with 49 vertical levels from the top to bottom of the ocean (1950 m depth).

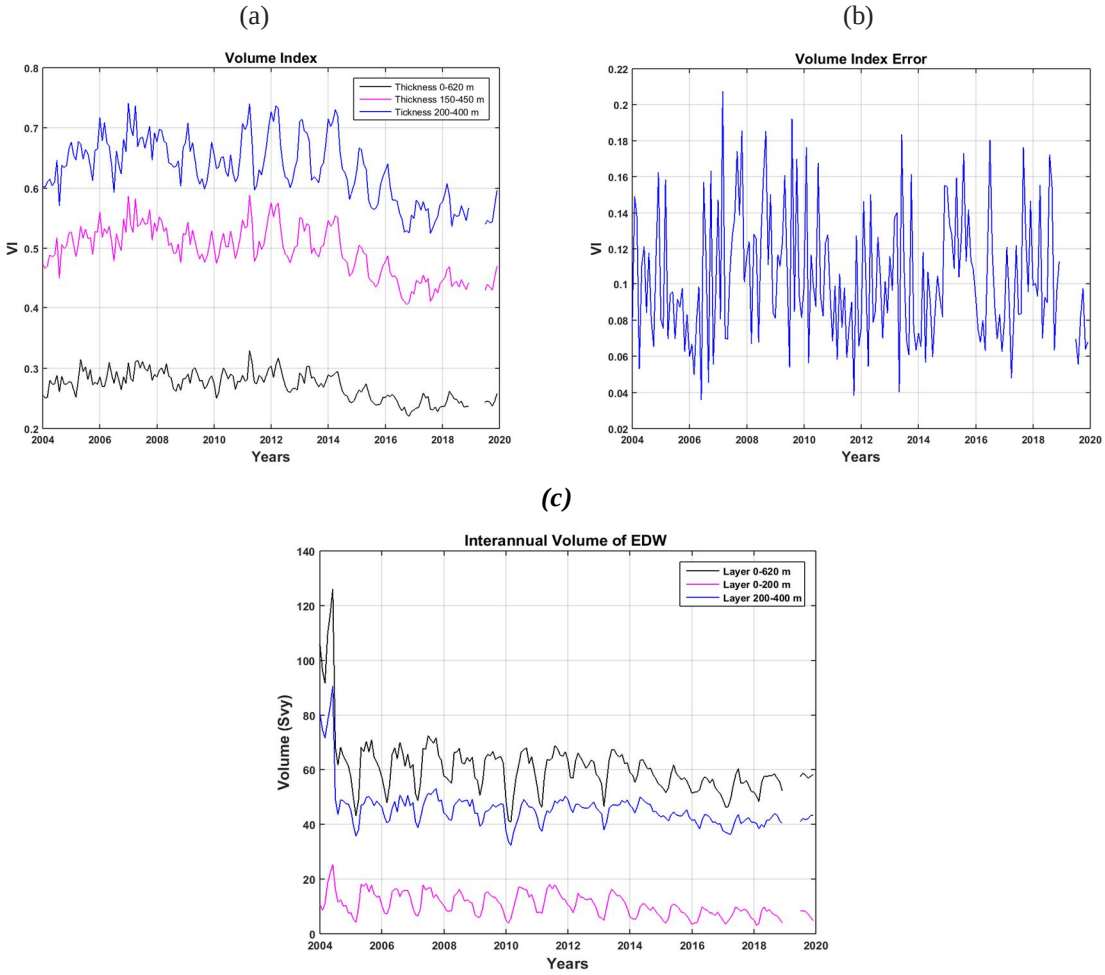

Fig. 4: Time series of the monthly average of the EDW volume index. From the top of the ocean to 620m depth, layer 0-620m depth (black line[-]), then from 150 m to 450 m depth, layer 150-450m depth (magenta line[-]), and finally layer 200-400m depth (blue line[-]).

The computations of the probability index after being monthly generated for each layer (from top to bottom) in our mathematical model, have then been multiplied by the volume of the corresponding layer, and finally have been integrated from the bottom within the domain of EDW. Fig.4c displays the monthly inter-annual Volume of EDW generated by our model. It shows three separated plots, the integrated volume of the layer from top to 620 m depth (black line), integrated from top to 200 m depth (magenta line), and integrated from 200 to 400 m depth (blue line). The three patterns have presented the same trend, displaying the seasonal cycle of EDW volume with a minimum in March and a maximum in June. The EDW total volume fluctuates around 60Svy with a maximum of 72Svy, the volume in the core layer (200-400 m) around 45Svy with a maximum of 51Svy and in the layer (0-200 m) around 10Svy with a maximum of 18Svy. We have noticed that the value of the volume in the year 2004 is biased by the higher number of profiles present this time.

In order to extract only the interannual signal, we have separated the initial signal into Seasonal cycle and low-frequency signal. For this, we have first calculated the average Annual cycle, and then we have subtracted it from the initial signal using the following formula:

$$V(t) = Vsc(t) + Vbf(t) + V0(t)$$

Where $V(t)$ total signal, Vsc is the Seasonal cycle, Vbf is low frequency or inter-annual anomaly signal, $V0$ is noise.

Figure 5 shows the monthly average anomaly of the EDW volume, which is an interannual signal of the EDW volume anomaly. We have observed a positive anomaly of the Volume in the year 2004 and values that oxalate around the normal (zero) from 2005 to 2014 with extremes in 2007-2008 (10Svy) and 2012 (8Svy), and a negative anomaly from 2015 to 2019 with a minimum in 2017 (-10*Svy*). The anomaly of EDW volume is in good agreement with the results that we have obtained previously, which showed a reduction in EDW volume from 2014 to 2019 [25]. The analysis also displayed the EDW volume has reached its largest increase at the end of 2007-2008 and its largest reduction in 2010 and 2017.

C. Seasonal variability of EDW using Volume Index

The seasonal variability of EDW volume has also been estimated by using the metric Volume Index. The study area is found in the Northern Hemisphere, which has four mean seasons. Authors have shown that EDW is ventilated by wintertime from January to March (JFM), where the EDW volume formation rate reaches the maximum at the end of March [10, 20, 23]. The seasonal variability of EDW volume was studied first by Kwon and Riser [20], and then by Forget et al.[6], which used three years of Argo profiles data interpolated by a general circulation model and showed a relative seasonal fluctuation around stable point. Forget et al. [6] estimated the seasonal cycle of winter increased the rate of EDW volume to 8.6Svy and the EDW total volume to 75Svy. Kwon and Riser [20] estimated the winter formation rate to be 3.93x1014 m3 / 12.47Svy. Billheimer et al. [33] studied the process of restratification and destruction of EDW. They analyzed their paper on the subducted EDW layer.

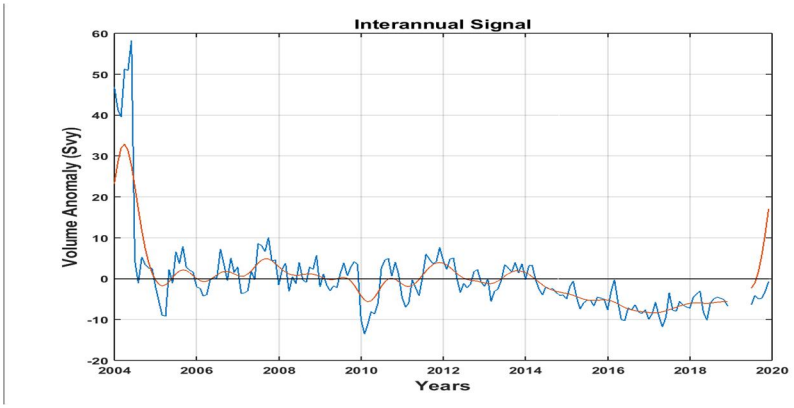

Fig. 5: Time series of the monthly average anomaly of the EDW volume (Inter-annual anomaly: blue line; three-month averaged signal: brown line).

In this paper, we have studied and analyzed the intra-seasonal variability of EDW volume by winter (JFM) and summer (JAS) time from 2004 to 2019 using the Volume Index method. Fig.6 displays the vertical profile of the EDW volume during the wintertime (a) and summertime (b). The seasons JFM and JAS have been extracted throughout the study period (2004-2019), and the seasonal time series of JFM (a) and JAS (b) were generated.

Globally, we have observed that EDW's total volume is greater (more voluminous) in the JAS season than JFM ones. The EDW vertical structure shows on one side, layers varying between 50m to 700m depth with a volume from 1Svy to 6.4Svy in summer, and on the other side layer varying between 150m to 700m depth with a volume from 0.5Svy to 6.4Svy in winter. The core of the EDW layer (depth 200-400m) has a higher percentage of probability of the presence of EDW in summer than in winter. There, Sublayers volume has stood at 3.5-6.4Svy in summer and by 2.5-6.4Svy in winter. The intra-seasonal analysis of EDW volume displays a good stratification of EDW as well in the winter season than in the summer ones, with a core, which is found between 200 m and 400 m deep. However, the signal of EDW in summer is scattered more widely than in winter. Intra-seasonal variability of EDW illustrated a slight increase from 2004 to 2007 in winter, but it was almost constant in summer during the same period. We also observed the reduction of the intra-seasonal signal from 2014 to 2019 in both winter and summer. Integration of all layers containing EDW has been done for both seasons after their volume has been multiplied by their weight point (probability). It has displayed in figure.7, the time series of EDW seasonal volume in winter (a) and summer (b) for the three patterns. Intra-seasonal variability of Volume has brought out results in affinity with EDW vertical structure analysis for the three patterns. This figure also shows that the EDW volume is greater in summer than in winter for the three patterns. The EDW total volume fluctuates around 65Svy with values varying between 55-72Svy in summer, while it is around 52Svy with values varying between 41-106Svy in winter. EDW core layer (200-400m) shows volume oxalate around 47Svy in summer with a maximum of 52.1Svy and minimum at 40Svy. However, it stands at 40Svy in winter with values varying between 32-80Svy. Finally, the layer (0-200m depth) displays volume varying between 6.9-18.5Svy in summer, while in winter it is by 3.1-11Svy.

(a) (b)

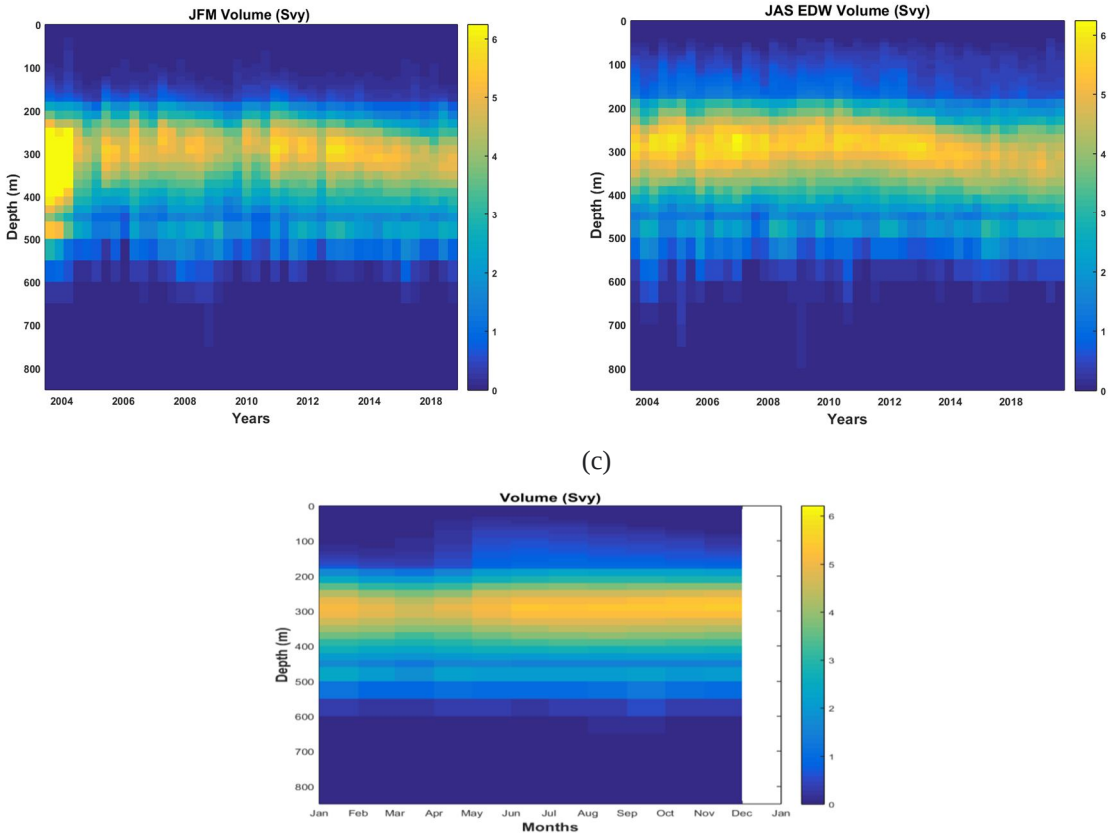

(c)

Fig. 6: Vertical profile of annual and the seasonal time series of the EDW Volume [season JFM (a), JAS (b), and Annual (c)] in the Subtropical North Atlantic (seasonal temporal series from 2004 to 2019). The Volume unit in Svy is indicated on the colorbar, ($1Svy=3.15*10^{13}$).

Bringing meaningful insight to the analysis of the EDW seasonal variability of JFM and JAS leads us to compare the two signals in terms of volume using a table and a graph (Table 1 and Fig. 8a). The JFM and JAS seasonal variability statistics for the EDW volume are shown in Table.1 from 2004 to 2019. In terms of volume, we have

(a) (b)

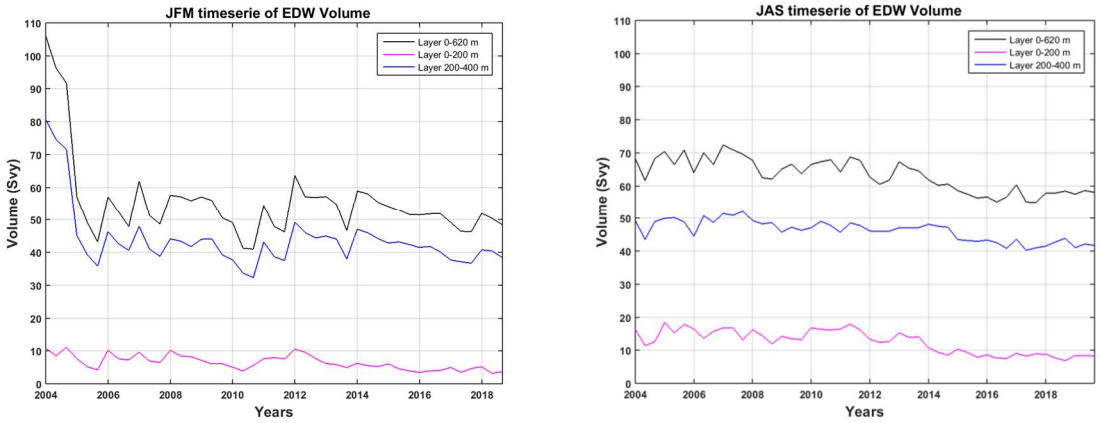

Fig. 7: Time series of seasonal EDW volume [season JFM (a) and JAS (b)]. From the top of the ocean to 620m depth, layers 0-620m depth (black line), then from 150 m to 450 m depth, the thickness of 150-450m depth (magenta line), and finally thickness of 200-400m depth (blue line).

(a) (b)

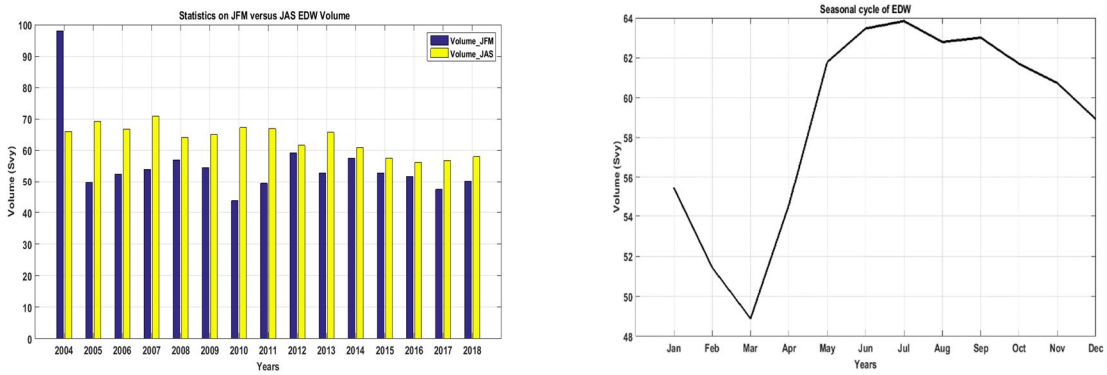

Fig. 8: Time series of seasonal (a) and annual (b) EDW volume [season JFM (blue bar) and JAS (yellow bar)] from 2004 to 2018. The volume is averaged over the three months January-February-March and July-August-September of each year. The Volume unit in Svy.

Observed from statistics that EDW is more important in season JAS than this of JFM, except in the year 2004. The JFM EDW volume ranges from 43 to 59 Svy and JAS from 56 to 71 Svy, following the same fluctuation patterns of the Volume Index. The volume is averaged for three months. The bar graph, Fig.8a for comparing the two season signals also displays the observing patterns. It shows in yellow that the JAS seasonal volume is higher than the JFM seasonal volume in blue. Our results are in agreement with the seasonal cycle of EDW volume represented in Fig.8b, which shows the JFM signal is lower than the JAS signal. The results of our analysis illustrated a signal of EDW volume higher in summer than in winter.

Table 1: Statistics displaying JFM and JAS seasonal variability of EDW Volume from 2004 to 2019. Second and fourth column VI (Volume Index) without unit, third and fifth column seasonal volume in Sverdrup.

	JFM		JAS	
Years	VI	V JFM	VI	V JAS
2004	0.2528	97.9865	0.2787	66.0836
2005	0.2640	49.8186	0.2936	69.2505
2006	0.2749	52.4894	0.2833	66.8411
2007	0.2897	53.9432	0.3017	70.9677
2008	0.2941	56.9022	0.2703	64.1109
2009	0.2826	54.5625	0.2748	65.1546
2010	0.2616	43.7545	0.2863	67.2557

2011	0.2824	49.5350	0.2823	66.9298
2012	0.2976	59.2040	0.2641	61.6461
2013	0.2845	52.8649	0.2767	65.7589
2014	0.2875	57.4765	0.2572	60.8683
2015	0.2604	52.9092	0.2429	57.4745
2016	0.2534	51.7117	0.2336	56.1407
2017	0.2331	47.2937	0.2385	56.8278
2018	0.2403	50.2064	0.2451	58.0469
2019	-	-	0.2442	58.0567

IV. DISCUSSION

The results of our analysis have demonstrated the total volume of EDW is more important (more voluminous) in summer (JAS) than in winter (JFM). The vertical structure of EDW has illustrated as well with interannual analysis as with seasonal analysis, the deepening of Mixed Layer (ML) from January to March, during the winter, and the restratification from April to June, and finally, another deepening from July to December. The monthly mean time series of the EDW has well displayed the signature of the seasonal thermocline on the vertical profile, which decays from June to March and increases from March to June, delimiting the upper mixed layer and EDW volume interior. Maze et al. [23] found this result in their paper by estimating the seasonal cycle of the mixed layer using potential vorticity. However, they studied the formation rate of EDW but did not analyze the total volume of EDW during winter and summer time. In the North Atlantic Subtropical region, by wintertime, upper waters are cold down by air-sea heat exchange due to severe atmospheric conditions (air buoyancy). This leads therefore to vertical mixing and the deepening of the mixed layer, which reaches the maximum size in March and breaks through the seasonal thermocline, ventilating the EDW core. This causes the EDW interior to increase in size and volume from March to June during the spring season, where restractification of the vertical water column takes place; we observe the formation of a seasonal thermocline, which reaches maximum development at the beginning of summer. This thermocline disappears again from autumn and plays an important role because improves vertical stratification, it slows down the mixing processes and the penetration of deep solar heat. Billheimer et al. [33] studied this process of restratification and destruction of EDW showing that EDW destruction starts at the top of the EDW layer in early summer and ends in late winter. Our results, consistent with Billheimers study, have shown that EDW total volume decreased from July to March and increase from April to June (Fig.4c and 6c). Billheimers work was focused on the destruction process of EDW and the seasonal cycle, but we have evaluated the total volume of EDW and its seasonal volume. The vertical profile of the EDW annual cycle also illustrates this seasonal variability of EDW volume (fig.6.c), displaying the signature of mixed layers throughout the year. The blue area on the top of our graphs (fig.3 and 6), which denotes the very weak presence of EDW could represent the mixed layer. It is just to let you see this signature. The seasonal thermocline usually separates the upper waters and STMW water in the North Atlantic Subtropical region, where some seasons mixed. Intra-seasonal variability of EDW seasonal volume has confirmed the same results.

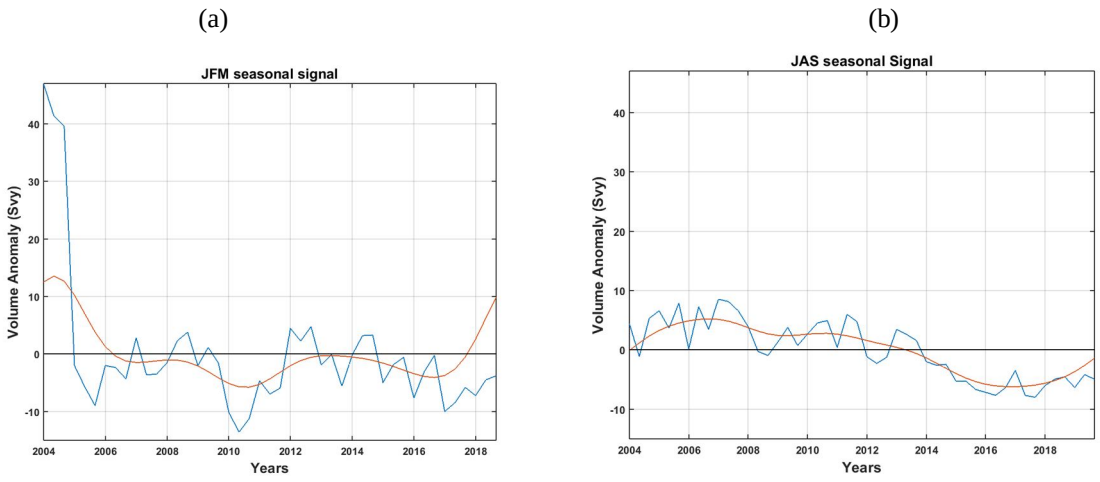

Fig. 9 Time series of the seasonal anomaly of the EDW volume index, [Season JFM (a) and JAS (b)] (Inter-annual anomaly: blue line; three-month averaged signal: brown line).

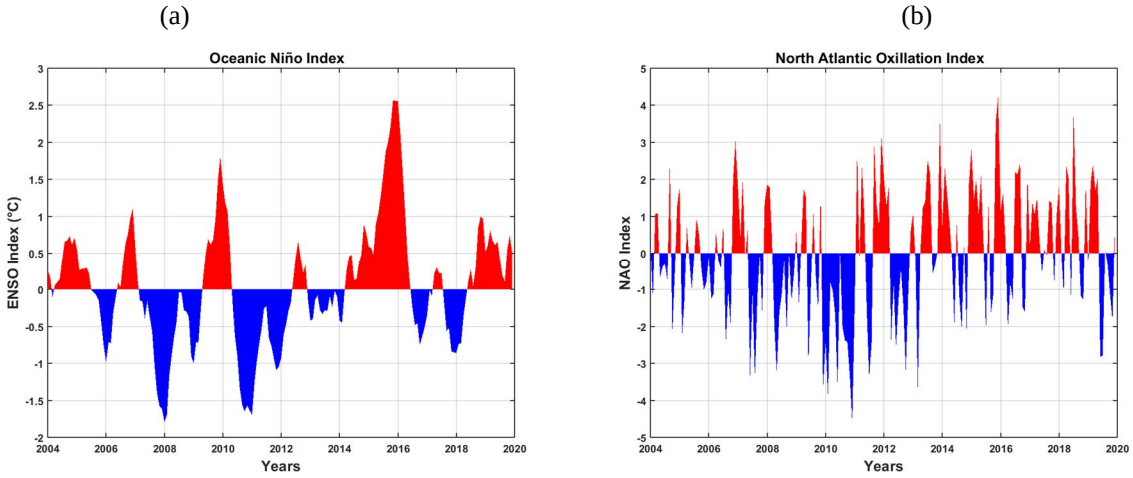

Fig. 10 Monthly anomaly in niño3.4 (a), monthly anomaly in North Atlantic Oscillation Index (b).

It shows that the EDW volume is greater in summer than in winter for the three patterns. The EDW total volume fluctuates around 65Svy in summer, while it is around 52Svy in winter. Billheimer et al. [33] investigated and quantified the destruction rates of the annual cycle of EDW, showing that the largest EDW intensities happen during FMA outcropping. But, we look into the other side by assessing not the destruction rate, but the total volume of EDW into the ocean during the JFM and JAS seasons. We compared the two signals in terms of volume. We observed that the EDW total volume is higher during the JAS season than during the JFM season.

As Billheimer et al. [33] the destruction rates of EDW start slower and steady in early winter and reach their highest rates during early summer. Our results illustrated what happens in the EDW volume interior. Billheimer's works investigated the mechanism of subducted EDW layer showing that the process of destruction rates of EDW is at the highest in early summer. Here, the EDW penetration is maximal leading the EDW total volume interior to be more important in summer than in winter as we have demonstrated in our study.

Forget et al. [6] estimated the seasonal cycle of EDW in volume formation rate. They evaluated the winter increase rate to 8.6Svy and the total volume to 75Svy using the OCCA dataset. Intra-seasonal variability of the winter season has reduced remarkably in the year 2010-2011. The volume of EDW was quite very weak during the winter season of 2011. This result is well in a good agreement with the work of Billheimer [34].

They explained that it was caused by weak buoyancy forcing, which gave way to shallower water than usual winter mixed layers throughout the subtropical vortex. We also noted that the downward trend in the intra-seasonal variability in winter and summer that we observed over the period 2014-2019 coincided with a negative anomaly in their volume (fig. 9 a and b). Inter-annual and intraseasonal variability analysis of EDW volume has displayed a downward trend during the period 2014-2019, that is the reduction of the EDW volume.

This event coincided with the very strong NAO+ that happened during the winter of 2013-2014 and El ÑINO ~nthat happened during the period 2014-2016 (figure.10a and b). The computed ~ correlation coefficient between NAO and EDW volume is -0.241 (p-value 0.3683), and -0.1789 (p-value 0.5054) with El ÑINO. The positive and negative phases of NAO ~ have some impact on EDW variability. We observe the positive phase of NAO could lightly be the cause of the reduction of EDW volume that occurred during the winter of 2013-2014.

We can see that the NAO index showed positive higher values during this period (figure.10b). In The same way, the weak volume of EDW observed in 2011 (the intra-seasonal variability) would come from the strong negative NAO during winter 2009-2010. EDW is ventilated during the wintertime, so the remarkable decline in EDW volume from 2014 to 2017 might be explained by the fact that the EDW zone was not enough ventilated by wintertime, as Billheimer et al. [34] demonstrated in their work. It might have been caused by weak buoyancy forcing, which in turn would indirectly come from the strong El ÑINO 2014-2016 that influences on the NAO event. Stevens et al. [25] found an 86 - 93% loss of EDW thickness in this region between 2010 and 2018, suggesting a gyre-wide signal reduction of EDW production.

Table 2: Correlation between NAO and annual EDW (column 2); winter EDW (column 4) and Summer EDW (column 7), n-pairs=16. The lag is negative when NAO leads EDW. Lines, 3 to 7, illustrate the time lags correlation from two earlier years (-2), one earlier year (-1), concurrent year (0), one previous year (1), and two previous years. The NAO index is averaged for the four months of DJFM.

	EDW		EDW-JFM		EDW-JAS	
Lags	R	P-value	R	P-value	R	P-value
-2	-0.2264	0.3991	-0.082	0.77	-0.3269	0.2165
-1	-0.1405	0.6038	-0.0096	0.97	-0.5254	0.0366
0	-0.2411	0.3683	0.084	0.76	-0.5472	0.0283
1	-0.3321	0.2088	0.1232	0.66	-0.2754	0.3019
2	-0.1494	0.5807	-0.3636	0.1827	-0.1738	0.5198

Correlations between total EDW volume and NAO-DJFM for different seasons (winter and summer) and annual years were calculated when NAO leads and lags EDW by 1-2 years (Table 2). Correlations were calculated over the common 2004-2019 EDW period with n pairs equal to 16 (see Table 2).Total EDW volume is anti-correlated with NAO during annual years and summer seasons for unprecedented lags. This correlation is significant (p - *values* < 0:05) in summer for the concurrent year (R = -0:5472*; lag* = 0) and a time lag of a previous year (R = -0:5254*; lag* = -1). the largest correlation occurring with a zero year lag in summer could imply that EDW responded best to the NAO signal during the concurrent year with perhaps 5-6 months memory of atmospheric forcing. The metric we used in this article, the Volume Index method, highlighted that the total volume of EDW is greater in summer than in winter. The total volume of EDW illustrated a significant anti-correlation with NAO in summer. We also discovered the results obtained by other authors. A decreasing trend was observed during the period 2014-2018, as Stevens et al. [25] found. Additionally, NAO could have been the cause of this downward trend in EDW volume.

V. CONCLUSION

The properties, characteristics and volume of EDW are a topic that has been widely studied by many authors [1{3, 5, 21, 23, 24]. Also, several works have been carried out on the variability of the EDW volume [6, 23, 25, 33]. In this paper, we explored the interannual, seasonal and intra-seasonal variability of the EDW using the Volume Index method. Our main objective was to quantify and compare the total volume of EDW in winter and summer. To compute and study the inter-annual and seasonal variability of EDW volume, Volume Index has been assessed focusing on the vertical integration of the oceans layer probability. This method is a metric based on a simple analysis of Argo in-situ vertical profiles of temperature, it is the vertical integral of the oceans layer probability of EDW. We have used the monthly objectively mapped BOA-Argo data from 2004 to 2019, with a 1◦ x 1◦ horizontal grid and 49 vertical levels from the surface to 1950 m depth. We analyzed the total volume of EDW in winter (JFM) and summer (JAS) and compared their signal. The main results of this paper demonstrate that the total volume of EDW is greater (more voluminous) in summer (JAS) than in winter (JFM). Our study showed that the total volume of the EDW fluctuates around 60Svy reaching its maximum at 72Svy. Furthermore, the total volume of the EDW fluctuates around 65Svy with values varying between 55-72Svy in summer, while it is around 52Svy with values varying between 41-106Svy in winter. It is important to note the higher number of profiles present in winter biases the volume value for the year 2004. The results of this article are in good agreement with the studies of Worthington and Forget [4, 6], who estimated the total volume of EDW to be approximately 75-80 Svy. Worthington et al. [4] published the first estimates of the volume of EDW, Kwon and Riser [20] estimated the winter formation rate at 12.47 Svy, Maze et al. [23] estimated the seasonal cycle of the mixed layer using the potential vorticity, Forget et al. [6] evaluated the seasonal cycle of the increase in winter rate of EDW volume at 8.6 Svy and total EDW volume at 75 Svy, Billheimer et al. [33] studied the restratification and destruction process of EDW and Li et al. [6] studied the extremes of EDW formation, showing that Ekman transport is an indicator of extreme EDW events. However, their work did not give an accurate estimate and difference in the total volume of EDW in winter and summer. We analyzed and evaluated the total volume of EDW in winter and summer using the VI method and showed that the volume of EDW is larger in summer than in winter. Billheimer's work studied the mechanism of the subducted EDW layer, showing that the process of EDW destruction rate is highest in early summer, where EDW penetration is maximum, this which leads the total interior volume of the EDW to be larger in summer than in winter, as we demonstrated in our study.

Interannual variability showed a slight increase from 2004 to 2008, a signal that oscillated around stability from 2008 to 2014, and a remarkable reduction from 2014 to 2019 as studied by Stevens et al. [25]. The volume index showed good stratification of EDWs in the ocean. NAO and El Ñino 2014-2016 were correlated with the reduction in EDW volume from 2015 to 2019. Intra-seasonal variability also showed a gradual reduction in EDW volume, from 2014 to 2019 in both winter and summer. It also showed a good correlation with NAO. We observed the weak signal of the EDW volume in winter, which was also well correlated with the NAO. The total volume of EDW illustrated a significant anti-correlation with NAO in summer.

Finally, the metric, the Volume Index method, was found to be an effective analysis tool for capturing EDW volume variability, with a statistical uncertainty of approximately 0.1. Therefore, we believe that this work has brought new insights for a better understanding of the EDW volume.

Data Availability Statements

The Work datasets are freely accessible online (links: see acknowledgments).

Declarations

There is no Funding

REFERENCES

[1] Worthington, L.V.: The 18 water in the sargasso sea. Deep-Sea Res. **5**, 297{305 (1959)
[2] Masuzawa, J.: Subtropical mode water. Deep-Sea Res. **16**, 463{472 (1969)
[3] Roemmich, D., Cornuelle:, B.: The subtropical mode waters of the south pacific ocean. J. Phys. Oceanogr. **22**, 1178{1187 (1992)
[4] WORTHINGTON, L.V.: On the north atlantic circulation. JOHNS HOPKINS UNIVERSITY PRESS, 110 (1976)
[5] MAZE, F.G.B.M.M.J.C.I. G.: Using transformation and formation maps to study the role of airsea heat fluxes in north atlantic eighteen degree water formation. J. PHYS. OCEANOGR. **39**, 1818{1835 (2009)
[6] FORGET, M.G.B.M..M.J. G.: Estimated seasonal cycle of north atlantic eighteen degree water volume. JOURNAL OF PHYSICAL OCEANOGRAPHY **41(2)**, 269{286 (2011)
[7] Speer, K., Forget, G.: Global Distribution and Formation of Mode Waters vol. 103, pp. 211{226. Academic Press., ??? (2013)
[8] Bingham, F.M..: Formation and spreading of subtropical mode water in the north pacific. J. Geophys. Res. **97**, 11177{11189 (1992)
[9] McCartney, M.S.: The subtropical recirculation of mode waters. s Mar. Res. **40**, 427{464 (1982)
[10] Hanawa, K., Talley, L.: Ocean circulation and climate-observing and modeling the global ocean; chapter 5.4 mode waters. Int. Geophys. **77**, 373{386 (2001)
[11] Roemmich, J.G.J.W.P.S. D., Ridgway, K.: Closing the time-varying mass and heat budgets for large ocean areas: The tasman box. J. Clim. **18(13)**, 457{473 (2005)
[12] Qiu, P.H.S.C.K.A.D.D.R.W.H.M.N.G.H. B., Jayne, S.R.: Observations of the subtropical mode water evolution from the kuroshio extension system study. J. Phys. Oceanogr. **36(3)**, 2330{2343 (2006)
[13] BATES, A.C.P.R.J.J. N. R., GRUBER, N.: A short-term sink for atmospheric co2 in subtropical mode water of the north atlantic ocean. NATURE **420(6915)**, 489{493 (2002)
[14] JENKINS, W.J., DONEY, S.C.: The subtropical nutrient spiral. GLOBAL BIOGEOCHEM. CYCLES **17)**, 1110 (2003)
[15] PALTER, M.S.L. J. B., BARBER, R.T.: The effect of advection on the nutrient reservoir in the north atlantic subtropical gyre. NATURE **437**, 687{692 (2005)
[16] FERNANDEZ, S.P..B.M. D.: Variability of the subtropical mode water in the southwest pacific. JOURNAL OF GEOPHYSICAL RESEARCH **122(9)**, 7163{ 7180 (2017)
[17] PENG, C.E.P.K.Y.-O..R.S.C. G.: Investigation of variability of the north atlantic subtropical mode water using profiling float data and numerical model output. OCEAN MODEL **13**, 65{85 (2006)
[18] WANG, V.B. X. H., SUN, Y.: Seasonal and inter-annual variability of western subtropical mode water in the south pacific ocean. OCEAN DYN. **65(1)**, 143{154 (2015)
[19] Jie, Y., Asher, W.E., Riser, S.C.: Rainfall measurements in the north atlantic ocean using underwater ambient sound. In: 2016 IEEE/OES China Ocean Acoustics (COA), pp. 1{4 (2016). IEEE
[20] KWON, Y.-O., RISER, S.C.: North atlantic subtropical mode water: A history of ocean-atmosphere interaction. GEOPHYS. RES. LETT. **31**, 1961{2000 (2004)
[21] TALLEY, M.E. L. D. RAYMER: Eighteen degree water variability. J. MAR. RES. **40**, 757{775 (1982)
[22] SUGA, H.K.T.Y. T.: Subtropical mode water in the 137-degrees-e section. J. PHYS. OCEANOGR. **19**, 1605{1618 (1989)
[23] MAZE, J. G. MARSHALL: Diagnosing the observed seasonal cycle of atlantic subtropical mode water using potential vorticity and its attendant theorems. J. PHYS. OCEANOGR. **41**, 1986{1999 (2011)
[24] MAZE GUILLAUME, M.J.T.A.-M.C.A.V.L. DESHAYES JULIE: Surface vertical pv fluxes and subtropical mode water formation in an eddy-resolving numerical simulation. DEEP-SEA RESEARCH PART II-TOPICAL STUDIES IN OCEANOGRAPHY **91**, 128{138 (2013)
[25] STEVENS SAMUEL W., M.G.B.N.R. JOHNSON RODNEY J.: A recent decline in north atlantic subtropical mode water formation. NATURE CLIMATE CHANGE **10(4)**, 335{341 (2020)
[26] Li, H., Xu, F., Zhou, W., Wang, D., Wright, J.S., Liu, Z., Lin, Y.: Development of a global gridded a rgo data set with b arnes successive corrections. Journal of Geophysical Research: Oceans **122**(2), 866{889 (2017)
[27] Gatz, D.F., Smith, L.: The standard error of a weighted mean concentrationi. bootstrapping vs other methods. Atmospheric Environment **29**(11), 1185{1193 (1995) [28] Gatz, D.F., Smith, L.: The standard error of a weighted mean concentrationii. estimating confidence intervals. Atmospheric Environment **29**(11), 1195{1200 (1995)
[28] Seitz, R.: Thermostad, the antonym of thermocline (1967)
[29] Schroeder, M.R.: Measurement of sound diffusion in reverberation chambers. The Journal of the Acoustical Society of America **31**(11), 1407{1414 (1959)

[30] Tsubouchi, T., Suga, T., Hanawa, K.: Comparison study of subtropical mode waters in the world ocean. Frontiers in Marine Science **3**, 270 (2016)
[31] Feucher, C., Maze, G., Mercier, H.: Subtropical mode water and permanent pycnocline properties in the world ocean. Journal of Geophysical Research: Oceans **124**(2), 1139{1154 (2019)
[32] Billheimer, S., Talley, L.D.: Annual cycle and destruction of eighteen degree water. Journal of Geophysical Research: Oceans **121**(9), 6604{6617 (2016)
[33] Billheimer, S., Talley, L.D.: Near cessation of eighteen degree water renewal in the western north atlantic in the warm winter of 2011{2012. Journal of Geophysical Research: Oceans **118**(12), 6838{6853 (2013)

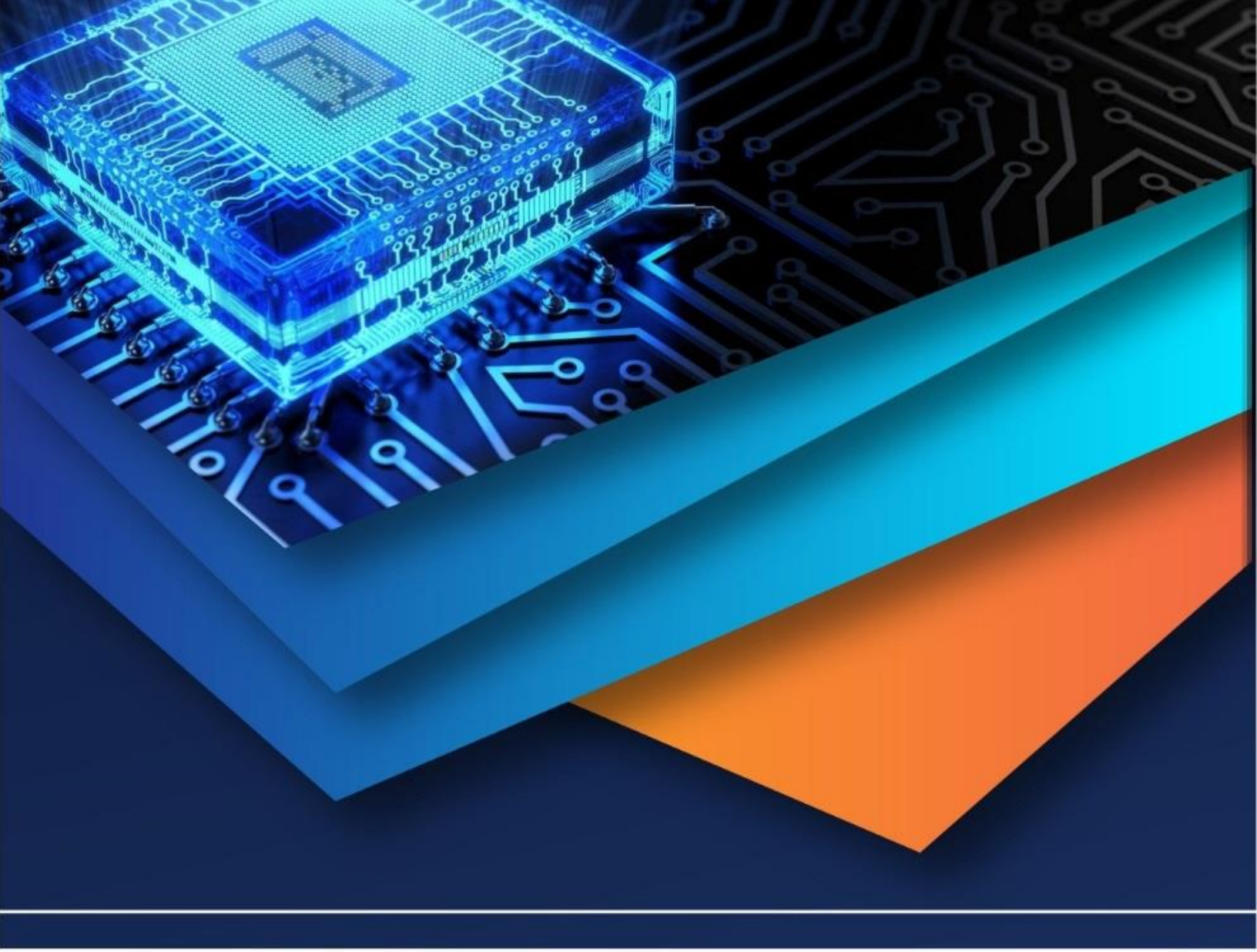

10.22214/IJRASET

45.98

IMPACT FACTOR: 7.129

IMPACT FACTOR: 7.429

INTERNATIONAL JOURNAL FOR RESEARCH

IN APPLIED SCIENCE & ENGINEERING TECHNOLOGY